ICONARP
International Journal of Architecture and Planning
Received: 06.06.2022 Accepted: 02.10.2022
Volume 10, Issue 2/ Published: 20.12.2022
Research Article
DOI: 10.15320/ICONARP.2022.220 E- ISSN:2147-9380
ICONARP

Reconsidering Urban Densification for Microclimatic Improvement: Planning and Design Strategies for Istanbul

Deniz Erdem Okumus*
Fatih Terzi**

Abstract

One of the key issues of the urban planning agenda is how urban density be decided in the spatial configurations of future neighbourhoods to overcome complex challenges such as urban warming. This paper aims to reconsider urban density as a spatial planning instrument to develop effective densification policies, planning and design strategies in terms of surface urban heat island (SUHI) mitigation in Istanbul. The quantitative research embraced a four-stage methodology including grid-based sampling design, decoding the taxonomy of urban density-matrix (UDM), land surface temperature mapping, and ANOVA tests. Tests were conducted on the UDM consisting of nine building typologies representing the horizontal and vertical urban density. The research indicated that the impact of urbanisation on SUHI can be mitigated by controlling densities and urban forms based on quantitative findings. The highest temperatures were recorded in areas with high-coverage-mid-rise and mid-coverage-mid-rise development. The different levels of SUHI in different building typologies having the same density indicated the mitigation potentials of the built-form in Istanbul's local urban warming. Low coverage and high-rise building forms were an optimal solution for mitigating SUHI in densely populated urban areas. The research gives insight into an ongoing debate among urban professionals in Istanbul concerning the impacts of density and the urban form for climate adaptation. It enables professionals to understand the impact of urban planning decisions on microclimate and integrate them into the operational processes. Considering quantitative research findings as a strong foundation for developing policy recommendations and using them as a guideline may create new opportunities for researchers, practitioners, and policymakers. The study has an original value for exploring design strategies to improve microclimate and promoting sustainable urban development.

Keywords:
Istanbul, spatial planning, urban density, urban design, urban heat island

*City and Regional Planning Department, Yildiz Technical University, Istanbul, Turkey (*Corresponding author*)
Email: denizer@yildiz.edu.tr

**Urban and Regional Planning Department, Istanbul Technical University, Istanbul, Turkey
Email: terzifati@itu.edu.tr

To cite this article: Erdem Okumus, D., & Terzi, F. (2022). Reconsidering Urban Densification for Microclimatic Improvement: Planning and Design Strategies for Istanbul. *ICONARP International Journal of Architecture and Planning,* 10 (2), 660-687. DOI: 10.15320/ICONARP.2022.220

INTRODUCTION

The population growth in cities (U.N., 2019) has brought bidirectional consequences of urbanisation: urban sprawl and urban intensification. While urban sprawl has caused changes in the land cover from natural to impervious and hard urbanised surfaces, urban intensification has increased the building density and created a more heterogeneous urban area with different urban geometries. These consequences triggered micro-climate issues such as local urban warming named the urban heat island (UHI) effect. UHI creates warmer urban areas with high surface temperatures compared to the rural and suburban surroundings (Hu, White, & Ding, 2016; Oke & Maxwell, 1975; Santamouris, 2013; Stewart & Oke, 2012; James A Voogt & Oke, 2003). Today, cities in different shapes and sizes around the world suffer from urban warming regardless of the climatic type. UHI intensity makes urban areas more vulnerable to the extreme climatic effects, particularly increases the heat stress during the heat waves which are more frequently occurred by global warming (Chow, Brennan, & Brazel, 2012; Santamouris, Ding, & Osmond, 2019). According to the latest reports of IPCC (2021, 2022), ongoing urbanisation trends with the increasing UHI effects will expose the urban areas to *more frequent, longer and warmer heatwaves*, enhance surface warming even towards rural surroundings and cause a new local warming crisis, particularly on minimum temperatures, as serious as global warming (IPCC, 2021, 2022). National/international climate targets particularly highlight the need for sustainable urban environments associated with rethinking the policies on the optimal use of urban space (Metz, Berk, den Elzen, de Vries, & van Vuuren, 2002; Pomponi, Saint, Arehart, Gharavi, & D'Amico, 2021; Swart, Robinson, & Cohen, 2003; Yilmaz, Irmak, & Qaid, 2022). The United Nations Sustainable Development Goals (SDGs), particularly goals of *'sustainable cities and communities'* (SDG.11) and *'climate action'* (SDG.13), emphasize the supplemental effect of microclimate actions on sustainable urban development and point out the localization of the concept through urban design strategies (U.N., 2015; U.N.D.P., 2015). Therefore, there is a strong need for exploring design strategies to improve microclimatic conditions by mitigating urban warming, and to promote sustainable urban development.

The urban planning and design fields take a critical approach to understand the key components of urbanisation that contributed to temperature variations and developing effective design strategies to prevent future crises in built-up environments through local warming mitigation. Recent research on the warming effects of three-dimensional urban geometry has identified urban density as a commonly referenced phenomenon of urbanisation (Guo, Zhou, Wu, Xiao, & Chen, 2016; Song et al., 2020; Sun, Gao, Li, Wang, & Liu, 2019; X. Yang & Li, 2015; Yin, Yuan, Lu, Huang, & Liu, 2018; Zheng et al., 2019; Zhou, Huang, & Cadenasso, 2011). As a microclimate response, reconsidering urban densification and reorganizing the heterogenic spatial structure of

DOI: 10.15320/ICONARP.2022.220

urban density have become a privileged strategy in urban metabolism to explore the density limitations of existing urban form and fabric (Knuth, Stehlin, & Millington, 2020). Hamin and Gurran (2009) refer to the exploration process as solving the "*density conundrum*" for urban cooling, whether designing a denser environment with a compact urban form or more open spaces with a sprawling urban form (Hamin & Gurran, 2009). The UHI literature includes multi-parameter evaluations (MPE) through various indicators as representative of vertical and horizontal urban density but most of them are not decision variables. The issue is that the MPE approach leads to an abstraction of understanding the effect of urban fabric elements on positive temperature anomalies. Literature needs an in-depth and site-specific reinvestigation on the impacts of building coverage (BC) and height (BH) as crucial spatial planning instruments and decision variables to develop effective densification policies in the planning and design practices. Therefore, throughout this study, the urban density phenomenon has been handled in two legs; horizontal building density represented by BC, and vertical building density which stands for BH captured by the *site-specific* maximum height of the building envelope (Alexander, 1993).

BC and BH variations have unequivocal effects on urban microclimate conditions and surface temperature anomalies due to the influences of solar radiation exposure, multiple reflections of solar radiation, natural ventilation and air circulation (Kleerekoper, Van Esch, & Salcedo, 2012; Liao, Hong, & Heo, 2021; Wong et al., 2011; Junyan Yang, Shi, Xia, Xue, & Cao, 2020). They bear the substantive cooling capacity, especially defined by the distances between buildings, in correlation with the other urban fabric components. UHI studies generally emphasize the strong promoting effect of BC and the reducing effect of BH on surface temperatures (Oke, 1987; Song et al., 2020; Sun et al., 2019; Yin et al., 2018; Zhou et al., 2011). Guo et al. (2016) revealed that lower building density and medium building height significantly caused a high land surface temperature (LST) variation in Guangzhou. Yin et al. (2018) explained that higher building densities create higher LSTs in Wuhan. Zheng et. al. (2019) demonstrated significant differences among districts with varied building densities and heights by analysing LST variations among residential areas in Beijing.

Despite the fact that there is a wealth of literature on the relationship between density and UHI, determining the appropriate density standards remains a challenge for practical urban planning strategies to minimise local urban warming. Therefore, we developed an extensive urban density-matrix (UDM), an instrument of the decision mechanism in the spatial planning system, that includes horizontal and vertical density units for a clear understanding of the relationship between UHI and urban densification. UDM approach promotes UHI mitigation regulations and local policies focusing on building urban densification standards in spatial planning practices. The current situation in the

ICONARP – Volume 10, Issue 2 / Published: 20.12.2022

cities demands that climate science be localised through urban design policies, guidelines, and design strategies based on quantitative research. According to Corburn (2009), the localisation of climate policies requires '*scientific facts*' (Corburn, 2009). It is obvious that only cities having scientific resources and quantitative findings will be able to develop such policies and design standards to improve built forms and design. Urban design standards, eventually codes, might easily find a place within the planning system especially in terms of local urban warming mitigation purposes through urban density control.

In this context, the purpose of this paper is to (1) utilize ANOVA tests to determine the statistical differences between the contributions of different building typologies in the UDM to UHI variations, and (2) develop concrete urban planning strategies focusing on density-based UHI mitigation. We believe that urbanisation's impact on urban warming may be minimised by controlling urban densities and urban forms, and we would like to discover if the optimal urban density and typology exist to regulate and mitigate the UHI effect. The quantitative findings will add to the current debate among urban professionals concerning the role of urban density in meeting climate goals. Istanbul is the case study on which we base our ideas, as the city offers a diverse range of densities for studying the effects of urban layout on heat island formation. Overall, we provide a reference to the localization of the SDGs (SDG.11,13) through design strategies focusing on reconsidering urban densification.

CONTEXT IN ISTANBUL

Istanbul, a megacity located in the Eastern Mediterranean climate zone, has been suffering from abnormally high urban temperatures (Dihkan, Karsli, Guneroglu, & Guneroglu, 2015). The outcomes of the unplanned urbanisation process induced by informal housing developments, enormous mass housing projects, and uncontrolled urban densification (Bolen, 2004; Keles, 1993; Terzi & Bolen, 2012) have triggered local warming and changes in micro-climatic conditions (Kaya, Basar, Karaca, & Seker, 2012). Even planned developments (high-rise and mixed-use projects in the city centre, and low-density sparse housing in the peripheries) have resulted in further heterogeneity in the urban fabric. Until recently, the city followed a linear development, mainly on the east-west axis without touching the borders of the northern forest areas and water basins. However, in the past decade, this traditional development pattern changed to a sprawl towards the north. This increase in the built-area also made a dramatic impact on the UHI effect and caused even higher temperatures (Basar, Kaya, & Karaca, 2008; Bektas Balcik, 2014; Ezber, Sen, Kindap, & Karaca, 2007; Kaya et al., 2012). The dispiriting urban warming trend in Istanbul requires us to rethink urbanisation for a policy remake of urban densification embracing effective UHI mitigation strategies.

DOI: 10.15320/ICONARP.2022.220

We consider two important limps for the urban warming problem in Istanbul: Underestimation of the local warming crisis and the UHI risks to heat stress by the local governmental authorities; lack of efficient and tangible urban planning strategies grounded in quantitative research findings on the correlation between UHI and urban density phenomena. Even though local governments have started to prepare various assessment reports on climate action plans and the factors contributing to climate change in the past couple of years (İ.B.B., 2018), the UHI issues are either not included or only mentioned peripherally in these reports. However, the city has a highly heterogeneous spatial layout with different levels of urban densities and building typologies which are unequivocally contributing to urban warming. Therefore, the city initially needs to investigate the effects of the building typologies based on urban density on the UHI formation for a policy remake on urban densification.

The urban density phenomenon is intrinsically a spatial planning instrument in the decision-making processes. The indicators of horizontal and vertical building density - building coverage and the maximum height of the building - are two main factors of spatial plans within the regulations of the urban planning system in Turkey. In the current situation, such metrics, which define the limitations of the structuring of the three-dimensional urban environment, are used to prioritise predominantly economic concerns. Spatial planning approaches without micro-climate concerns promote unplanned densification and heterogeneity in the urban area, which eventually leads to a significant rise in the graphic of temperature variations in the urban area (Feng & Myint, 2016; F. Yang, Lau, & Qian, 2010; Yin et al., 2018; Zheng et al., 2019). Therefore, the planning authorities should consider the UHI effects in spatial planning decisions based on urban densification to reduce urban warming and achieve climate-sensitive urbanisation.

MATERIALS AND METHODS

This study was conducted in 4 basic stages, each with its sub-steps: (1) *grid-based sampling design*, (2) *decoding the taxonomy of UDM*, (3) *LST mapping*, and (4) *Univariate analyses of variance: ANOVA tests* (Figure 1). The paper proposed an UDM based on the horizontal and vertical building density to provide a better understanding of the relationships between urban warming and density phenomena for the case of Istanbul.

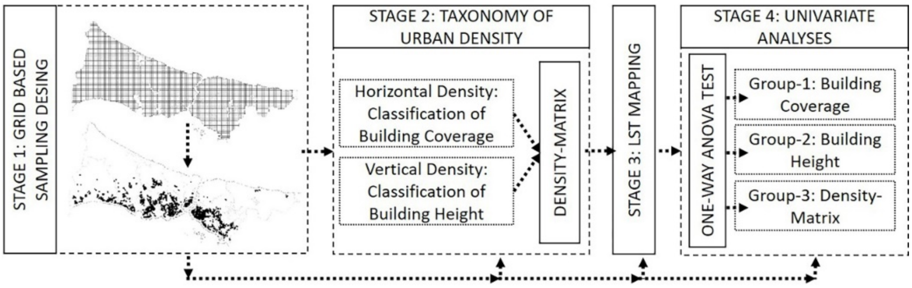

Figure 1. Research design scheme.

Study Area and Grid-Based Sampling Design

Istanbul is located in the northwest of the country and spans the divide between the European and Asian continents, a quality that gives the city unique characteristics (Figure 2). The coastal city also occupies the transition zone between the Sea of Marmara and the Black Sea, and takes advantage of the natural ventilation potential of the Bosphorus Strait and its complex topography (Ç.Ş.B., 2018). Approximately 27% of Istanbul is covered by urbanised areas (Figure 2).

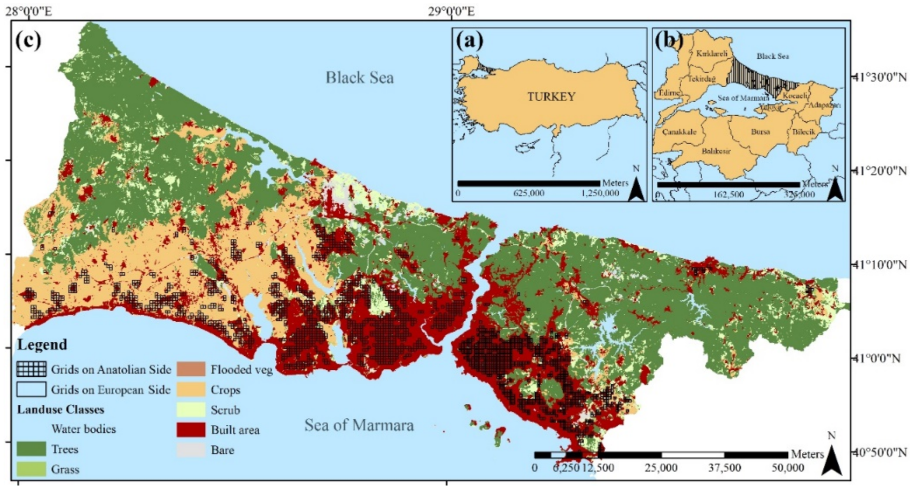

Figure 2. The location of the study area in Turkey (a), in Marmara Region (b) and the sample grid cells in Istanbul (c). Sample grids are shown on the 2020 land cover map which was produced and shared freely by ESRI.

The grid-based sampling method was adopted to represent different urban fabrics in the study area. First, the provincial borders of Istanbul were divided into sample grid cells at a resolution of 500x500m which is approximately a neighbourhood size. The grid elimination method of four basic criteria was then implemented to remove the influences of uncontrollable factors: Removing (a) cells containing water masses, or those with no buildings, (b) cells less than 1km from a large water mass, (c) cells located within forests or valleys and (d) cells with over 25% slope coverage. Thus, the sample size was reduced to 1949 grid cells – 1265 located on the European and 684 located on the Anatolian side (Figure 2). The 1949 grids represent the unique morphologies of Istanbul, which were developed by diverse social and economic drivers in different eras (Masoumi, Terzi, & Serag, 2019; Terzi & Bolen, 2009, 2012).

DOI: 10.15320/ICONARP.2022.220

Decoding the Taxonomy of Urban Density-Matrix

Regarding the UDM, building coverage ratio (BCR) and building height (BH) are numerical measurements that refer to the planning codes in the planning system and built-up features of the city. The operations here were based on the analysis of spatial characteristics in 1949 sample grid cells through the codifying taxonomy of the UDM. The vector-based building geodatabase was obtained from the CAD-source city map produced in 2017 by Istanbul Metropolitan Municipality. Buildings were identified into sample grid cells, and each cell was considered as a parcel of intersecting buildings to calculate the BCR and BH. The BCR was calculated as the ratio of the total footprint occupancy to the area of the grid cell. BH captured the average height of the building envelopes in the grid cell. Both the BCR and the BH were classified as *High/Mid/Low Coverage* and *High/Mid/Low Rise* in the density-matrix. Nine typologies comprising the cross-referenced classes of BCR and BH were employed in the UDM (Table 1). For instance, HighCoverage-HighRise (HCHR) defines the areas with a BCR between 0.51-1, meaning the building stock covers over half of the parcel. HCHR also includes the arrangement of buildings over 21-meters in height, meaning that the building stock is over 7 storeys. MidCoverage-MidRise (MCMR) indicates areas BCR ranging between 0.25-0.50 and mid-rise buildings of between 12-21 meters in height (building stocks between 4-7 storeys) (Table 1).

Table 1. The taxonomy of urban density.

Taxonomy	Typology	Code	Definition
Building Coverage (BC)	HighCoverage	HC	1.00 ≥ BCR ≥0.51
	MidCoverage	MC	0.50 ≥ BCR ≥0.25
	LowCoverage	LC	BCR <0.25
Building Height (BH)	HighRise	HR	BH >21 m
	MidRise	MR	21 m ≥ BH ≥12 m
	LowRise	LR	12 m > BH
Urban density-matrix (UDM)	HighCoverage-HighRise	HCHR	1.00 ≥ BCR ≥0.51 ; BH >21 m
	HighCoverage - MidRise	HCMR	1.00 ≥ BCR ≥0.51 ; 21 m ≥ BH ≥12 m
	HighCoverage - LowRise	HCLR	1.00 ≥ BCR ≥0.51 ; 12 m > BH
	MidCoverage - HighRise	MCHR	0.50 ≥ BCR ≥0.25 ; BH >21 m
	MidCoverage - MidRise	MCMR	0.50 ≥ BCR ≥0.25 ; 21 m ≥ BH ≥12 m
	MidCoverage - LowRise	MCLR	0.50 ≥ BCR ≥0.25 ; 12 m > BH
	LowCoverage - HighRise	LCHR	BCR <0.25 ; BH >21 m
	LowCoverage - MidRise	LCMR	BCR <0.25 ; 21 m ≥ BH ≥12 m
	LowCoverage - LowRise	LCLR	BCR <0.25 ; 12 m > BH

Land Surface Temperature Mapping

LST variations and anomalies were used as proxy indicators of the surface urban heat island (SUHI) effect. The thermal remote sensing method for LST mapping allows the observation of the surface energy balance and can produce more accurate models at multiple spatial scales. The spatial distribution of LST is affected by urbanisation patterns and surface characteristics (Arnfield, 2003; Bektas Balcik, 2014; Mirzaei & Haghighat, 2010; Quattrochi & Goel, 1995; James A Voogt & Oke, 2003; Weng, 2009). However, it is important to note the probability of a cloudy sky, the difference between observed surface temperature and air temperature, and the limitations of any vertical or horizontal structures within urban areas (Mirzaei & Haghighat, 2010).

In the Mediterranean climate region, SUHI rises to a peak in the summer season due to the high levels of solar radiation (Arnfield, 2003; Oke, 1982; Salvati, Roura, & Cecere, 2017). The effect of urbanisation on Istanbul's local climate is further exacerbated during the summer months because wind speeds are at a minimum (Ezber et al., 2007). Moreover, in 2017, the highest annual temperature and daily hours of sunshine were recorded in the July months (M.G.M., 2022). Therefore, Istanbul's LST was mapped by using the Landsat-8 OLI/TIRS satellite image of July 25, 2017, with 0% cloud cover (The satellite image was recorded for 1 minute between 08:43-08:45). The Operational Land Imager (OLI) sensor of Landsat-8 consists of nine bands at 30m resolution (the panchromatic Band 8 is at 15m resolution), and the Thermal Infrared Sensor (TIRS) has two thermal bands (Band 10-11) at re-sampled 30m resolution (collected at 100m resolution). Band-10 (10,60-11,19) was used as a single spectral band (Guha, Govil, Dey, & Gill, 2018) in this study due to concerns about the calibration uncertainty of Band-11 (11,50-12,51) for quantitative analyses and retrieval of LST values (USGS, 2019).

The Landsat-8 images were operated on with the following image processing steps. (1) Converting the digital numbers of pixels to the top of the atmosphere's reflectance (Barsi et al., 2014). (2) Transforming the band data to brightness temperature (Xu & Chen, 2004). (3) Calculating the Normalized Vegetation Index (NDVI), Proportion of Vegetation (PV), and Land Surface Emissivity (Jiménez-Muñoz, Sobrino, Gillespie, Sabol, & Gustafson, 2006; Jiménez-Muñoz et al., 2009; Sobrino, Jiménez-Muñoz, & Paolini, 2004; Weng, Lu, & Schubring, 2004). (4) Calculating LST. Due to the limited number of monitoring stations in Istanbul's settlement area, LST values could not be verified by in situ measurements. Therefore, LST anomaly values (LSTa) calculated according to the average temperature of the urbanised area were used in the statistical analyses.

Univariate Analyses of Variance: One-Way ANOVA Post Hoc Testing

One-way analysis of variance, a method to compare means of and identify the specific differences between more than two groups, was used to demonstrate whether there are statistically significant differences between building typologies in density-matrix in terms of their contributions to the SUHI variations. ANOVA tests were iterated in three groups, BC (Group-1), BH (Group-2), and the taxonomy of the UDM (Group-3), to detect the difference between the LSTa means. Before analysing the differences, we tested two assumptions of ANOVA that are normality and homogeneity of variance (HOV) between groups to determine whether it was appropriate to use ANOVA. Analytical and graphical examinations through Kolmogorov–Smirnov tests, histograms,

DOI: 10.15320/ICONARP.2022.220

Q-Q plots, and boxplots of LST variations were applied for normality testing. HOV tests calculated the Levene statistic to control the equality of group variances. The assumptions (equal variances assumed) were satisfied to use ANOVA associated with the HOV test results in which sig.>0.05. Since ANOVA results showed that there is a significant difference between groups with sig.<0.05, one-way ANOVA tests were conducted through post hoc tests based on Scheffé's Method. Scheffe's examines linear combinations of group means and compares all possible pairs in unequal sample sizes (Scheffe, 1953, 1959). We conducted Sheffe's post hoc tests in three groups, in which group-1 was for BC typologies (with subgroups of HC-MC-LC), group-2 was for BH (with subgroups of HR-MR-LR) and group-3 was for UDM with seven subgroups (Table 1).

RESULTS

Land Surface Temperatures in Istanbul

The LST map showed that the large water bodies surrounding the coastal city, Istanbul, provide a certain level of reduction in the UHI effect. Even though the surface temperatures were lower in the coastal zone than in the inner parts of the city through the proximity to large water bodies, this cooling effect could not be maintained over long distances towards the inner city due to high urban densities (Figure 3). Particularly, the high-density urbanisation of the southern part of Istanbul eliminated any cooling effect from the Sea of Marmara. Because the northern parts of the city are mostly covered by natural surfaces such as water basins, forests, and agricultural areas, and as they also benefit from the cooling effect of the Black Sea, their surface temperatures remain lower than those found within the southern districts. The higher surface temperatures in the south part (the most urbanised and industrialised area) than in the north indicated that the distribution of LST is directly related to the urbanisation pattern in Istanbul (Figure 3). However, surface temperatures tended to increase in certain northern regions due to the new transportation hubs and residential developments.

Surface temperatures in Istanbul ranged between 22.03°C and 47.76°C, and the temperature difference between urban and rural areas was 4.29°C on 25th July 2017. Even if the average LST was 30.40°C in Istanbul, the urban average was 34.73°C (Figure 3). According to the long-period statistics, the average temperature is 25.8°C, the maximum is 30.9°C and the minimum is 21.6°C in July in Istanbul (M.G.M., 2022). Surface temperature statistics (min-max-average values) above the long-period averages confirmed the urban warming in July 2017. The highest surface temperature, nearly 16°C above the maximum long-term average, signalled a significant warming crisis in Istanbul.

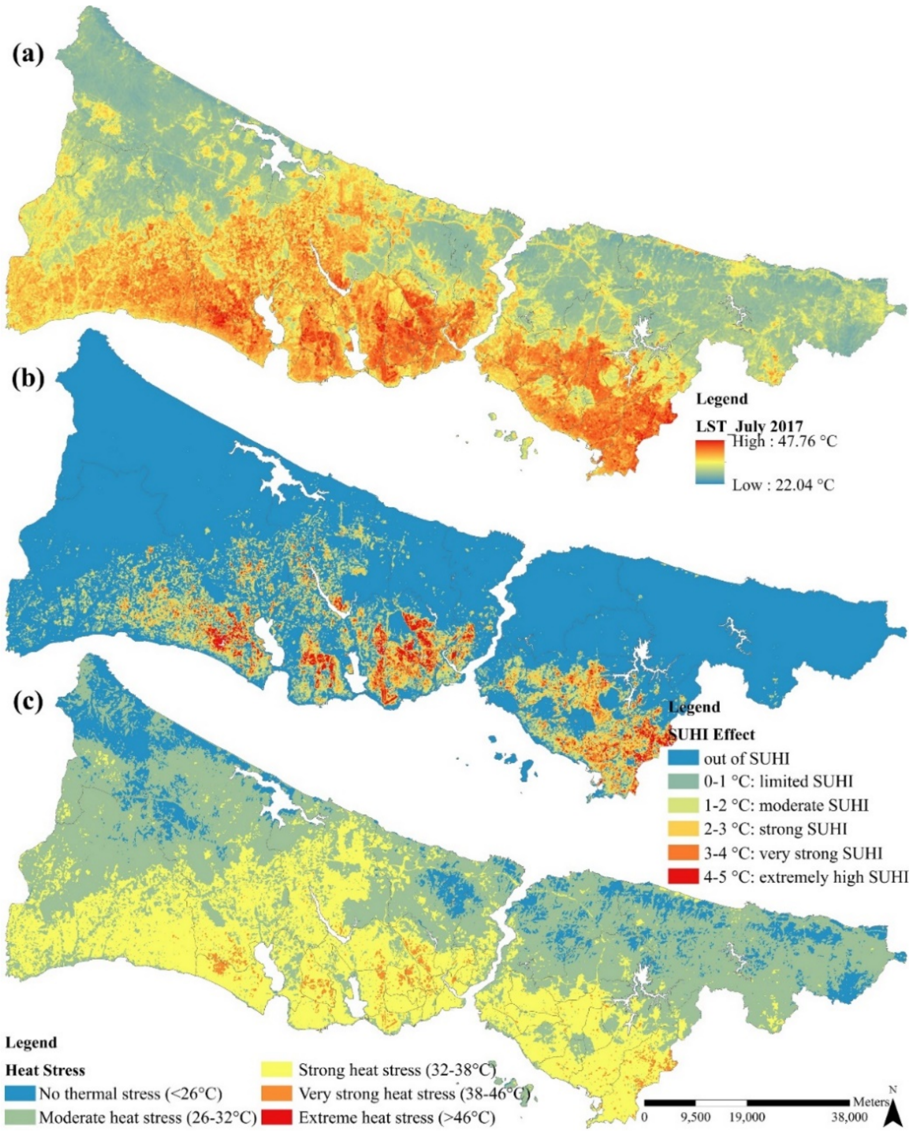

Figure 3. LST distribution (a), maps of SUHI effect (b) and heat stress (c) of Istanbul on 25th July 2017. (a) was produced from Landsat-8 thermal image. (b) and (c) were extracted from LSTs. (b) indicates the LST anomalies above the urban average as a proxy of the SUHI effect. (c) was classified as for Błażejczyk et. al. (2013)'s thermal stress categorisation.

While the LSTa below 34.73°C showed the non-SUHI effect, surface temperatures above the urban average indicated the potential SUHI effect (Figure 3). The natural northern parts were generally out of the SUHI effect with surface temperatures below the urban average. However, LST anomalies reached 5°C in the inner and high-density parts of the city and indicated an extremely high SUHI effect (Figure 3). 51% of the built-up area had a SUHI effect at various levels. Accordingly, the built-area's 16% was under the limited (LSTa: 0-1°C) and 14% was under the moderate (LSTa: 1-2°C) SUHI effect. Although temperature anomalies of 2°C are considered as extreme heat events on a global scale, limited and moderate SUHI effects might be minimised by minor interventions such as increasing urban vegetation in urban space. However, minimising the LSTa above 2°C, strong-very strong-extremely high SUHI effects requires structural interventions in the urban fabric such as reconfiguration of urban density and form (Erdem Okumus & Terzi, 2021). In Istanbul, 12% of the built-area was subject to a strong SUHI effect (LSTa: 2-3°C), 10% was subject to a very strong (LSTa: 3-4°C), and 5% was subject to an extremely high (LSTa: 4-5°C) SUHI effect.

DOI: 10.15320/ICONARP.2022.220

Since the humidity rate in coastal cities is higher than in the inner settlements, heat stress increases with the combination of humidity and SUHI and reaches a critical level. In Istanbul, strong SUHI effects intensified in the urbanised areas, creating very strong heat stress but also putting even rural parts under strong heat stress (Figure 3). According to Blazejczyk et al. (2013), temperatures over 26°C indicate thermal heat stress and temperatures over 32°C show strong heat stress (Błażejczyk et al., 2013). While Istanbul's 89% was under heat stress, 97% of the built-up area had moderate or strong heat stress. Another critical finding that explains the severity of the urban warming issue in Istanbul was that 65% of Istanbul's lands, which had not yet encountered the SUHI effect, are under heat stress at various levels.

Density Typologies and Spatial Distributions in Istanbul

The heterogeneous urban fabric in Istanbul includes various urban forms and geometries based on building density (Figure 4). Findings demonstrated that horizontal and vertical building densities are higher on the European side than on the Anatolian side. The BCR is lower on the Anatolian side due to the dominance of residential land use. High coverage typologies intensify in the city centre of the European side, and the BCR values decrease significantly away from the centre towards the peripheries for both sides. Contrarily, high-rise typologies are concentrated on the peripheries, mostly covering mass housing units. City centres are dominated by mid-rise typologies for both sides (Appendix 1).

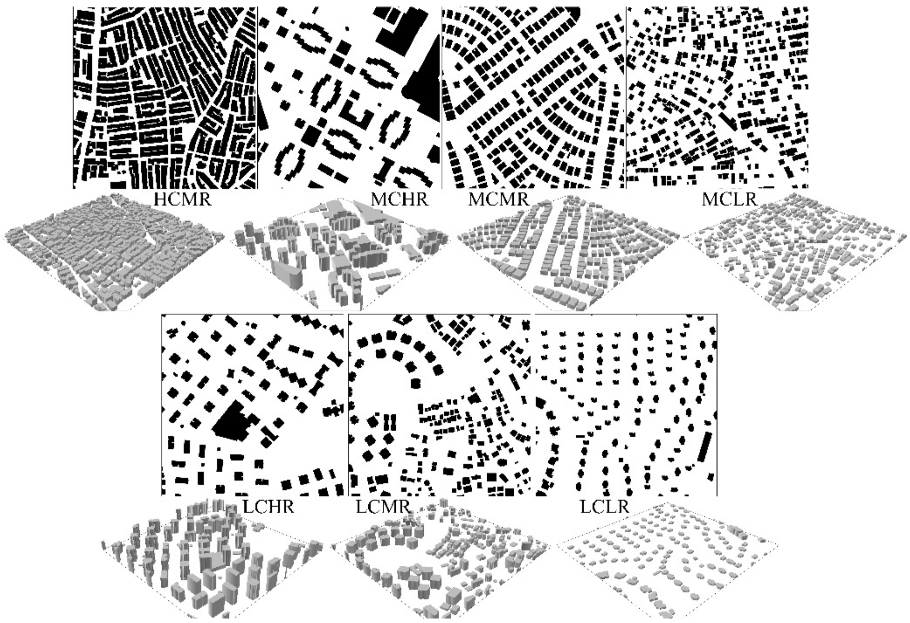

Figure 4. 2D/3D views from sample layouts of building typologies in UDM. Morphological form of long-linear building arrays in HCMR unfastens to distributed molecular form towards the LCLR typology.

The spatial distribution of the UDM supports the bidirectional development process in Istanbul: the construction of lower horizontal and vertical density areas in the peripheries; the higher horizontal density redevelopment of the city centre (Appendix 1). The findings showed that Istanbul's urbanised area has 7 types of building typologies

–HCMR, MCHR, MCMR, MCLR, LCHR, LCMR, LCLR- in the UDM (Appendix 1, Table 2). The typologies of HCHR and HCLR could not be identified in Istanbul. 44% of the grid cells are LCLR, 20% are MCMR, 19% are LCMR, 7% are MCLR, 6% are LCHR, 3% are HCMR and 1% are MCHR, respectively. The most prevalent morphologies in Istanbul are low-coverage and low-rise, the molecular form of urban sprawl towards semi-urban zones (Figure 4). Mid-coverage-mid-rise and low-coverage-mid-rise morphologies share the second rank. The mid-coverage and high-rise array is the least common typology, with only 6 grid cells. High-coverage and mid-rise morphology consisting of long-linear building arrays existed in 63 grid cells and concentrated on the European side (Figure 4).

Table 2. Descriptives of building typologies in Istanbul.

	Code	N	$BCR_{max.}$	$BCR_{min.}$	$BH_{max.}$	BH_{min}	$FAR_{max.}$	$FAR_{min.}$
BC	HC	63	0.62	0.51	18	12	3.22	1.89
	MC	531	0.50	0.25	30	3	3.64	0.35
	LC	1355	0.24	0.10	51	3	2.71	0.10
BH	HR	127	0.43	0.10	51	24	3.64	0.10
	MR	830	0.62	0.10	21	12	3.24	0.10
	LR	992	0.46	0.10	9	3	1.50	0.10
UDM	HCHR	0*	NA	NA	NA	NA	NA	NA
	HCMR	63	0.62	0.51	18	12	3.22	1.89
	HCLR	0*	NA	NA	NA	NA	NA	NA
	MCHR	6	0.43	0.28	30	24	3.64	2.19
	MCMR	394	0.50	0.25	21	12	3.24	0.93
	MCLR	131	0.46	0.25	9	3	1.50	0.35
	LCHR	121	0.24	0.10	51	24	2.72	0.10
	LCMR	373	0.24	0.10	21	12	1.80	0.10
	LCLR	861	0.24	0.10	9	3	0.88	0.10

N: Number of grid cells regarding the stated typology in 1949 sample grids.
FAR (Floor area ratio): one of the density metrics that indicate the construction rights in the urban regulatory planning system, is detected by the formula: (BCR*(BH/3)/ParcelArea).
* Typologies are not available in 500x500m grid resolution in Istanbul.

Surface Temperatures in Urban Density Typologies

Temperatures at the HC typologies were highest during the day, ranging between 35.50 and 39.24°C. The LST_{mean} was around 37°C and resulted in a 2.63°C temperature anomaly on average which indicates a strong SUHI effect in HC areas. Temperature conditions led to strong heat stress dominantly; however, there were grid cells experiencing very strong heat stress in HC typology. Similarly, the MC areas also recorded strong heat stress caused by temperatures between 32.27 - 38.70°C. The MC typology created a moderate SUHI effect at 1.08°C of LSTa. The LC areas tended to be cooler with mean temperatures of 34.20°C, which is very close to but lower than the urban average. The $LST_{max.}$ at 38.79°C demonstrated that there were LC neighbourhoods having a strong SUHI effect as outliers. Even though LST_{mean} in LC grid cells presented no SUHI effect, strong and moderate heat stress was identified in LC neighbourhoods (Table 3, Appendix 1, Figure 5).

DOI: 10.15320/ICONARP.2022.220

Table 3. Surface temperatures of building typologies in urban density.

ANOVA Groups	Code	$^*LST_{2017max}$	$^*LST_{2017min}$	$^*LST_{2017mean}$	*SUHI ($LSTa_{2017mean}$)	Std. Dev.
Group-1: Building Coverage (BC)	HC	39.24 °C	35.50 °C	37.36 °C	**2.63 °C**	0.99
	MC	38.70 °C	32.27 °C	35.81 °C	**1.08 °C**	1.28
	LC	38.79 °C	26.18 °C	34.20 °C	-0.53 °C	1.60
Group-2: Building Height (BH)	HR	37.86 °C	31.60 °C	33.69 °C	-1.06 °C	1.00
	MR	39.24 °C	27.98 °C	35.24 °C	**0.51 °C**	1.61
	LR	38.79 °C	26.18 °C	34.46 °C	-0.27 °C	1.77
Group-3: Urban density-matrix (UDM)	HCHR	NA	NA	NA	NA	NA
	HCMR	39.24°C	35.50 °C	37.36 °C	**2.63 °C**	0.99
	HCLR	NA	NA	NA	NA	NA
	MCHR	37.86 °C	33.05°C	35.54 °C	**0.81 °C**	1.42
	MCMR	38.70 °C	32.27 °C	35.82 °C	**1.09 °C**	1.35
	MCLR	38.15 °C	32.57 °C	35.80 °C	**1.07 °C**	1.05
	LCHR	35.96 °C	31.60 °C	33.58 °C	-1.15 °C	0.87
	LCMR	37.79 °C	27.98 °C	34.27 °C	-0.46 °C	1.28
	LCLR	38.79 °C	26.18 °C	34.26 °C	-0.47 °C	1.77

* Statistics show the average values of grid cells related to the specific typology.

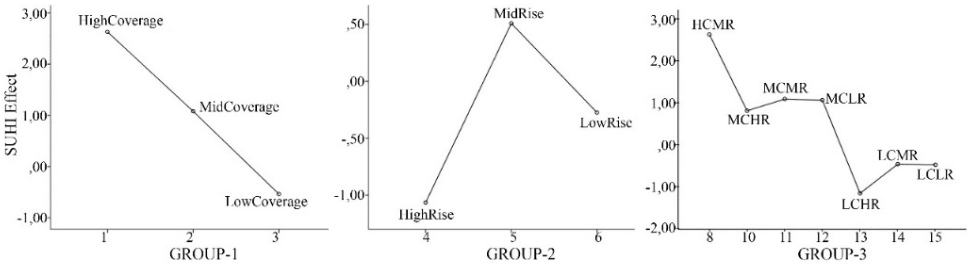

Figure 5. SUHI effect ($LSTa_{2017mean}$) plots of BC (Group-1), BH (Group-2) and UDM (Group-3).

In the group of building heights, the MR was the unique typology, creating a limited SUHI effect with a positive temperature anomaly on average. However, high LSTmax values in the BH typologies stated that there still might be neighbourhoods creating strong SUHI effects individually. There was a downward trend in the average temperatures of the HR typologies. Moreover, the HR areas were the coolest typology in the BH group, with around 1°C below the urban average. Similar to the BC group, BH typologies were under the dominant effect of moderate and strong heat stress (Table 3, Appendix 1, Figure 5). Throughout the UDM typologies, the highest temperature anomaly was detected in the HCMR areas with a strong SUHI effect. While MCMR and MCLR areas had moderate effects, neighbourhoods with the MCHR typology embodied a limited SUHI effect. Temperatures were lower in LCHR, LCMR and LCLR typologies and LCHR were the lowest (Table 3, Figure 5).

ANOVA Test Results

Analytical and graphical analyses of normality tests and the results of the Levene statistic regarding HOV testing met the requirements to apply ANOVA examination in this study. Varying temperatures of typologies in the UDM directly affected the normal distribution graph. Particularly, MCMR had both a wider range and a higher average temperature value. However, MCHR had a narrower range and lower LST_{mean} than other MC typologies. While MCMR typologies led to the highest LST variation, MCHR created the lowest temperature variation in Istanbul. In LC typologies, LCLR had a wider range but LCMR had a higher LST_{mean}. Even though the frequency distributions of UDM did not entirely overlap with the normal curve, typologies were close enough to a normal distribution with p-values >0.05 (Figure 6).

According to the ANOVA post hoc tests, even though significant differences were detected between some subgroups, a few typologies appeared to have similar effects on SUHI formation. Initially, tests showed that each BC and BH typology has a distinct influence on the SUHI effect (sig. 0.05). The biggest differences appeared between the HC and LC typologies in the BC group (mean diff.: ±3.16; sig.:0.00). While the HC typology created a warming trend in the neighbourhoods, LC assisted in a decrease in temperature anomalies. In the BH group, the test proved that the mean difference is significant between HR and MR pairs (mean diff.: ±1.57; sig.:0.00). HR typology resulted in the lowest anomalies below the urban average, but MR contributed to increasing the SUHI effect (Appendix 2). According to adj. R2 values of univariate analysis, BC emerged as a more efficient and stronger indicator for SUHI examinations than BH (adj. R^2_{BC}: 0.25; adj. R^2_{BH}: 0.07).

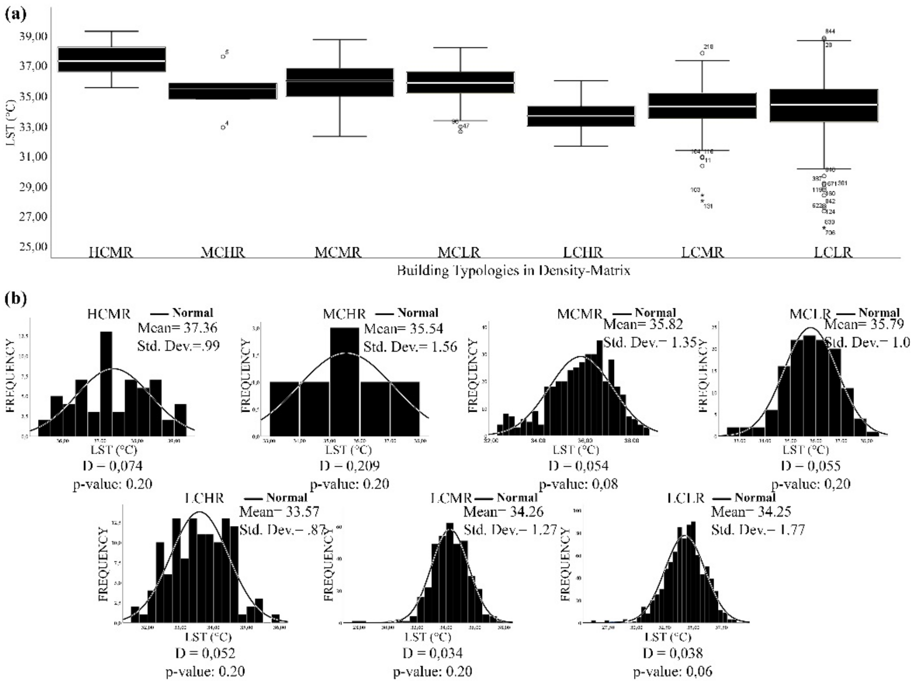

Figure 6. LST distributions (a) and frequency distributions (b) of UDM typologies (Landsat-8, 25th July 2017). (a) was produced according to the taxonomy of density-matrix in Istanbul (average temperature is 34.73°C). (b) demonstrates the typologies in UDM with a normal distribution line and the results of Kolmogorov-Smirnov normality test. The variable is normally distributed if p-value > 0.05.

Throughout the UDM typologies in group-3, the highest difference appeared between HCMR and LCHR pairs (mean diff.: ±3.79; sig.:0.00). While HCMR created a strong SUHI effect with the highest departure from the urban average of LST, the lowest LST was detected at LCHR with the temperature far below the urban average. HCMR demonstrated differences at various levels with other typologies, except MCHR. Because HCMR and MCHR typologies had similar effects (sig.: 0.23) on LSTa in Istanbul, densification decisions in urban space based on HCMR or MCHR typologies have identical effects on urban warming. Indeed,

DOI: 10.15320/ICONARP.2022.220

MCHR did not have any particularly unique effect among the UDM typologies (sig. values>0.05). MCMR, on the other hand, distinguished itself not only from HCMR but also from LCHR (mean diff.: 2.25; sig.: 0.00), LCMR (mean diff.: 1.55; sig.: 0.00), and LCLR (mean diff.: 1.57; sig.: 0.00). The highest difference in MCMR occurred in LCHR. In addition, MCLR had dissimilar effects on HCMR (mean diff.: 1.57; sig.: 0.00), LCHR (mean diff.: 2.22; sig.: 0.00), LCMR (mean diff.: 1.53; sig.: 0.00), and LCLR (mean diff.: 1.54; sig.: 0.00); the highest difference score was obtained with LCHR.Since the effects of MCLR were similar to those of MCHR and MCMR, the same coverage ratios seemed to create similar impacts on urban warming. However, it is not the same for low coverage fabrics (Appendix 2). The findings contribute significantly to urban planning and design strategies relating to urban densification and the selection of appropriate building typologies, with the goal of reducing urban warming through SUHI mitigation.

DISCUSSION

Density-Matrix Approach in Evaluating SUHI Impact of Urbanisation

Density is not only an instrument of certain policies followed by spatial planning but also a common concept in measuring the environmental impacts of urbanisation. Varying urban development dynamics create different densification patterns in cities, horizontally and/or vertically. The heterogeneous spatial structure of building typologies formed based on urban densification policies creates substantial consequences in terms of SUHI formation. Our findings strongly emphasised that different typologies of horizontal and vertical densification in UDM produce varied levels of temperature anomalies. A comprehensive framework of UDM helped both evaluate the SUHI impacts of horizontal and vertical densification patterns and breed the combinatorial solutions of building typologies based on UDM classes, in terms of SUHI mitigation. Such combinatorial solutions can offer alternative solutions for SUHI mitigation with different density trials, instead of producing a single solution in urban neighbourhoods. The matrix also provides an input to urban planning practices by facilitating the urban density distribution on the city having complex development dynamics.

The important gap in the UHI-density literature is that the low, medium and high-density categories have non-standardised ranges that vary depending on the characteristics of the city in each research. For example, a high-density perception in Oklahoma City, USA, could be interpreted as medium or even low density in Istanbul. Because of this relativity, cross-comparisons for comprehending the UHI-density relationship remain limited. The UDM shows the quantitative ranges of both horizontal and vertical density classes, resulting in an adaptable framework for cities around the world with varying cultures and urban development dynamics. This approach paves the way for similar studies

ICONARP – Volume 10, Issue 2 / Published: 20.12.2022

that consider both horizontal and vertical density, as well as the development of more concrete, effective, and density-based heat island mitigation strategies.

SUHI Impacts of Building Typologies in Density-Matrix

Empirical analyses indicated both the contribution of urbanisation on SUHI formation in terms of urban density in Istanbul and the differentiating effects of building typologies in the heterogeneous spatial structure of the city. Even though almost each of the horizontal and vertical densification typologies in the density-matrix has an independent effect on SUHI formation, findings highlighted that building coverage is a more efficient and stronger indicator for SUHI studies than the building height (Guo et al., 2016; Liao et al., 2021; Yin et al., 2018). BCR had a higher relationship with LST than BH in Istanbul. Attempts for SUHI mitigation in Istanbul might take the advantage of the robust impact of BCR in the neighbourhoods.

The positive linear relationship between BCR and LST anomalies (Guo et al., 2016; Liao et al., 2021; Yin et al., 2018) promotes decreasing building coverage to mitigate the SUHI in Istanbul's neighbourhoods. According to the researchers, the increasing tendency in LST with higher building coverage is based on concerns of fewer green spaces and poor ventilation in the neighbourhoods (Liao et al., 2021; Yin et al., 2018). Low BCR values possibly provide larger open green spaces and sparsely distributed urban layout design supporting the airflow, and weaken the SUHI effect (Yin et al., 2018; Zhao, 2018; Zhou et al., 2011). Ventilation and green coverage were not directly subjected to this study, but the decreasing trend in surface temperatures in the low coverage typology might be caused by the cooling effects of the large vegetative surfaces and the accelerated heat loss due to the gratifying airflow in sparsely built-areas in Istanbul. More likely, since the Landsat's transit time is during 08:43-08:45 when the sun just rises, low temperatures occurred in the areas with low building coverage typologies might be due to the nocturnal cooling effect of the high sky openness (Arnfield, 1990a). Contrarily, the greater potential of absorbing solar radiation through a large number of roof surfaces and lower radiation reflectance from street surfaces possibly led to higher surface temperatures in medium and high coverage areas (Chun & Guldmann, 2014; X. Yang & Li, 2015).

Even though studies have asserted that building height has a negative relationship with LST (Zheng et al., 2019), a non-linear mechanism was detected between building height and LST anomalies in Istanbul. Guo et al. (2016) supported the non-linear relationship between urban morphology and LST variations even if they indicated the positive correlation between BH and LST. For the case of Istanbul, MR typologies produced the highest surface temperatures among the BH classification (Guo et al., 2016; Lin, Lau, Qin, & Gou, 2017). Potentially, having more vegetative coverage and promoting airflow inside the neighbourhood

DOI: 10.15320/ICONARP.2022.220

explain the lowest contribution of HR typologies to the SUHI effect (Feng & Myint, 2016; Zheng et al., 2019; Zhou et al., 2011). Moreover, tall buildings provide a large amount of shading which might influence the behaviour and intensity of SUHI (F. Yang et al., 2010). Researchers declared that site shading conditions are directly related to day-time LST variations and SUHI effects, and explained that the shadows formed by HR buildings decrease temperatures and heat island intensity by creating a cooling effect (Guo et al., 2016; F. Yang et al., 2010).

Findings highlighted that the highest temperature values were recorded in HCMR areas among the typologies in density-matrix. HCMR typology creates high horizontal and vertical density neighbourhoods including enclosed urban areas surrounded by buildings, attached-long row city blocks and mostly hard and impervious pavements (Figure 4). In comparison to other typologies, its deeper canyon geometry, lower level of sky visibility, less ventilation capacity produces a significant effect on SUHI intensity by determining the amount of solar radiation that can reach and be absorbed in urban surfaces (Hu et al., 2016; Oke, 1987; Shishegar, 2013; F. Yang et al., 2010; Yin et al., 2018). On the other hand, the lowest LSTa were recorded in LCHR typologies in Istanbul. Areas with lower horizontal densities, sparsely distributed buildings and larger open spaces produce the highest levels of sky visibility and a uniform canyon geometry. A few researchers emphasised that as the depth of canyon geometry increases and the visibility of the sky decreases, the heat island effect may tend to decrease due to the limited exposure of the surfaces to solar radiation (Arnfield, 1990b; Giridharan, Lau, Ganesan, & Givoni, 2007; Strømann-Andersen & Sattrup, 2011). Contrary to this, Oke (1981) and Hu et al. (2016) revealed that urban temperatures tend to increase in such districts due to the impediment to cooling of the urban surfaces caused by buildings having high horizontal and vertical density and lower levels of sky visibility (Hu et al., 2016; Oke, 1981).

Contributions to the Micro-Climate Sensitive Planning and Design Strategies

Herein, we discuss the contributions to the design strategies regarding SUHI mitigation. Rethinking the overall urban densification policies while renewing built-up areas and developing new urban areas helps to control the temperature anomalies and promotes the reduction of local warming. The findings demonstrated that high-building coverage creates higher temperature anomalies; therefore*, decreasing horizontal density with a lower building coverage ratio helps to mitigate UHI effects significantly*. One of the design strategies to reduce the SUHI effect in neighbourhoods is to develop residential areas by keeping the BCR below 0.50. This means that the building footprint covers less than half of the parcel. To keep the SUHI effect even lower, the BCR should be kept below 0.25.

ICONARP – Volume 10, Issue 2 / Published: 20.12.2022

In areas with high land values, where building rights must be preserved to ensure construction feasibility (e.g., in or near the city centre), the design combination of a lower horizontal density (BCR<0.25) and a higher vertical density (BH>21 meters) provides the optimal solution for mitigating SUHI. While prior research has demonstrated that increasing building height can help lower LST in residential areas (Zheng et al., 2019; Zhou et al., 2011), this study discovered a nonlinear relationship between BH and LST. MCHR and LCHR are the two typologies that resulted in a reduction in the density matrix's LST anomalies. The minimal impact of high-rise and low-coverage urban areas on surface temperatures demonstrates their potential for heat islands (Gago, Roldan, Pacheco-Torres, & Ordóñez, 2013). The second design strategy, here, is based on lowering the building coverage, and it is formulated as the *combination of low building coverage and high building height within the density matrix's building height limitations.* We explain the relatively better results of LCHR than LCLR as the horizontal density of the LCHR model (the distance between buildings is much greater) compared to the LCLR model: in other words, there are fewer buildings per unit area.

In urban renewal practices, there may be market pressure to enhance construction rights in terms of project feasibility, particularly in or near the city centre. The demand of local stakeholders to preserve or expand economic assets puts pressure on increasing urban density both horizontally and vertically in attempts to renew the urban area. Under such market pressure, we might be able to give a picture of what configurations might be utilised to reduce local warming without compromising existing development rights while also renewing built-up areas. Despite the constant but high construction rights in built-up areas, regulating the spatial configurations of building typologies can nevertheless decrease the SUHI impact. Different amounts of SUHI impact in different building typologies might all be referring to the same construction rights. For example, when re-building urban areas using HCMR urban fabric, it may be preferable to use MCHR or LCHR typologies. The quantitative outcomes of this investigation showed that whereas HCMR produces the greatest LSTa, MCHR and LCHR contribute less to the temperature anomalies. Despite having almost the same land development rights as the HCMR type, surface temperatures in LCHR urban areas were significantly lower. Various amounts of the SUHI impact are generated by urban areas with the same development rights but different building forms and typologies.

The third design strategy is formulated as *designing high-rise buildings but with higher distances between them.* The height and coverage (as a proxy for the distance between buildings) of the buildings are strong structures controlling the wind direction and speed which is an important cooling factor in the urban area (He, Ding, & Prasad, 2020b, 2020a; Jun Yang et al., 2019). High-rise buildings and low building coverages with larger spaces between buildings provide a

DOI: 10.15320/ICONARP.2022.220

preferred situation in the summer month by increasing windiness and allowing the surface temperatures to drop. This built-form also increases thermal comfort in the outer environment and reduces the energy demands for cooling indoors. However, the wind is an undesirable factor in winter. Increasing the cooling effect with the wind may cause a decrease in thermal comfort and an increase in the energy demand for heating. Therefore, taking the advantage of promoting wind to minimise urban warming in the summertime might cause disadvantageous ventilation conditions in wintertime (Kleerekoper et al., 2012).

Design strategies for urban spatial development might provide heat loss presumably by enhancing airflow and/or ventilation conditions, creating more shadowed surfaces and enabling more open spaces for urban vegetation coverage (Kleerekoper et al., 2012; Yilmaz, Külekçi, Mutlu, & Sezen, 2021; Yin et al., 2018). It should not be forgotten that local characteristics are significant for the efficiency of such standards, which might lead to conflicting situations. For instance, Kleerekoper et al. (2012) specified for the Netherlands that designing urban areas in compact built form might be preferable for temperature mitigation due to the fewer heat storage capacity of fewer facades. However, even though the design of the deep street canyon with high-rise buildings and narrow streets obstruct the overheating, it minimises natural ventilation and increases the energy demand for heating in the wintertime by creating dark shadows (Kleerekoper et al., 2012; Wong et al., 2011). Another example, Pomponi et al. (2021) supported the idea that taller buildings are better for the environment when having the urban layout design (building footprints) perspective since they present optimal use and maximal efficiency of space and prevent urban sprawl. However, they also stated that high coverage low rise urbanisation might be more environmentally friendly than vertically denser patterns from a perspective of the construction tall and heavier structures with carbon-intense building materials (Pomponi et al., 2021).

This paper reveals the limits of what building height and footprint cause how much surface warming effect, from the urban densification perspective. Hereby, we need to state that while low coverage typologies might cause urban sprawl in metropolitan areas resided high populations, vertical development associated with the high-rise typologies raises concerns about damaging human scale perception, breaking street-building relationships, and ruining the image, identity and culture of the city. Therefore, the spatial organisation of density-dependent typologies and urban density distributions should be optimised to both minimise urban warming and eliminate the abovementioned concerns. Moreover, controlling urban density is not highlighted as the most powerful strategy to minimise urban warming in this study. Even if the urban density is strongly correlated with LST, any single morphological factor is not enough to minimise urban warming related to the heat island effect. It is also not claimed that the urban fabric with high-rise blocks with a low coverage ratio is the best morphological design for Istanbul's neighbourhoods. We need to mention that the strategy based on reducing BCR should be applied with the maximum building height (hmax.) limitation. The reduction of horizontal density allows vertical densification to the extent of the existing construction area. Due to the hmax boundary, it may not be possible to produce the density levels suggested by this research in all neighbourhoods with HC and MC in Istanbul. Besides that, any structural modification might not be applied to the urban fabrics located in Istanbul's historical centre or in the regions with high historical value. In such cases, minor improvements, such as increasing vegetation coverage, help to improve urban micro-climate (Erdem Okumus & Terzi, 2021).

Technical Limitations

Directional variations in observed temperatures are among the technical limitations of the study. Using the thermal image for a certain date might cause the anisotropy effect of urban surface temperatures (James A Voogt & Oke, 1997, 1998; James Adrian Voogt, 1995). The downward trend at the temperatures in the areas with especially HR typologies and the shadow impact might also be related to the anisotropy effect of LST extracted by satellite images. As the sun angle is too low at the time the image was recorded, LST trends depending on BH are directly affected by the anisotropy effect. The effect might be eliminated by using another thermal image recorded at different periods, however, there is not another thermal image on July 25, 2017, recorded by Landsat-8. Therefore, the study remained within the limitations of the anisotropy effect.

CONCLUSION

One of the key issues of the urban planning agenda is how urban density be decided in the spatial configurations of future neighbourhoods to overcome complex challenges such as urban warming. Herein, reducing urban warming is essential motivation by examining and rearranging the urban densities through the comprehensive UDM approach presented in this study. The significance of this paper lies in the urban density concept and providing tangible contributions to urban reconstruction in Istanbul.

This paper indicated the possibility of mitigating SUHI by reorganizing urban spatial configurations on a density basis and assisting policy decisions using quantitative measurements. Surface temperature anomalies become more apparent when UDM typologies are considered. Variable spatial layouts of urban communities based on the combination of varying horizontal and vertical density levels can modulate the LSTa-measured urban warming. Horizontal density has a greater effect on variations in LST than vertical density does. While horizontal density was positively correlated with LSTa, vertical density

DOI: 10.15320/ICONARP.2022.220

had a non-linear relationship with LSTa. Urban areas with a high density of buildings and a medium building height resulted in a much higher LST. In comparison, the lowest LST values were found in districts with low coverage and high-rise buildings. Additionally, spatial configurations with equal construction permissions but varied building typologies generate distinct SUHI values. While urban density is a critical topic for SUHI research, densification strategies should not be regarded as a stand-alone tool for mitigating urban warming. Any intervention that integrates additional morphological and urban fabric aspects has a high probability of achieving SUHI minimisation with high efficiency.

Urban density, which includes building coverage and height, is also a critical aspect of Turkey's urban regulatory planning system since it helps define the three-dimensional urban environment's boundaries. We propose that Istanbul's local warming be mitigated by using of density as a control mechanism. Decisions about urban densification should be developed in line with SUHI impact studies during the planning and design processes.

Overall, analysing the effects of different building typologies and densities on SUHI enables urban planners and designers to better understand the impact of urban planning/design decisions on microclimate elements and to develop ways to mitigate UHI effects. Considering quantitative research findings as a strong foundation for developing policy recommendations and using them as a guideline may create new opportunities for researchers, practitioners, and policymakers.

ACKNOWLEDGEMENTS/NOTES

This paper was produced from the PhD thesis conducted by the corresponding author under the supervision of the second author. The study conception and design were supported by the Scientific Research Projects Department of Istanbul Technical University, Istanbul, Turkey [grant number 42088]. The final manuscript has been completed by the support of the Scientific and Technological Research Council of Turkey (TUBITAK), 2214-A International Research Fellowship Program for Ph.D. Students.

ICONARP – Volume 10, Issue 2 / Published: 20.12.2022

APPENDICES

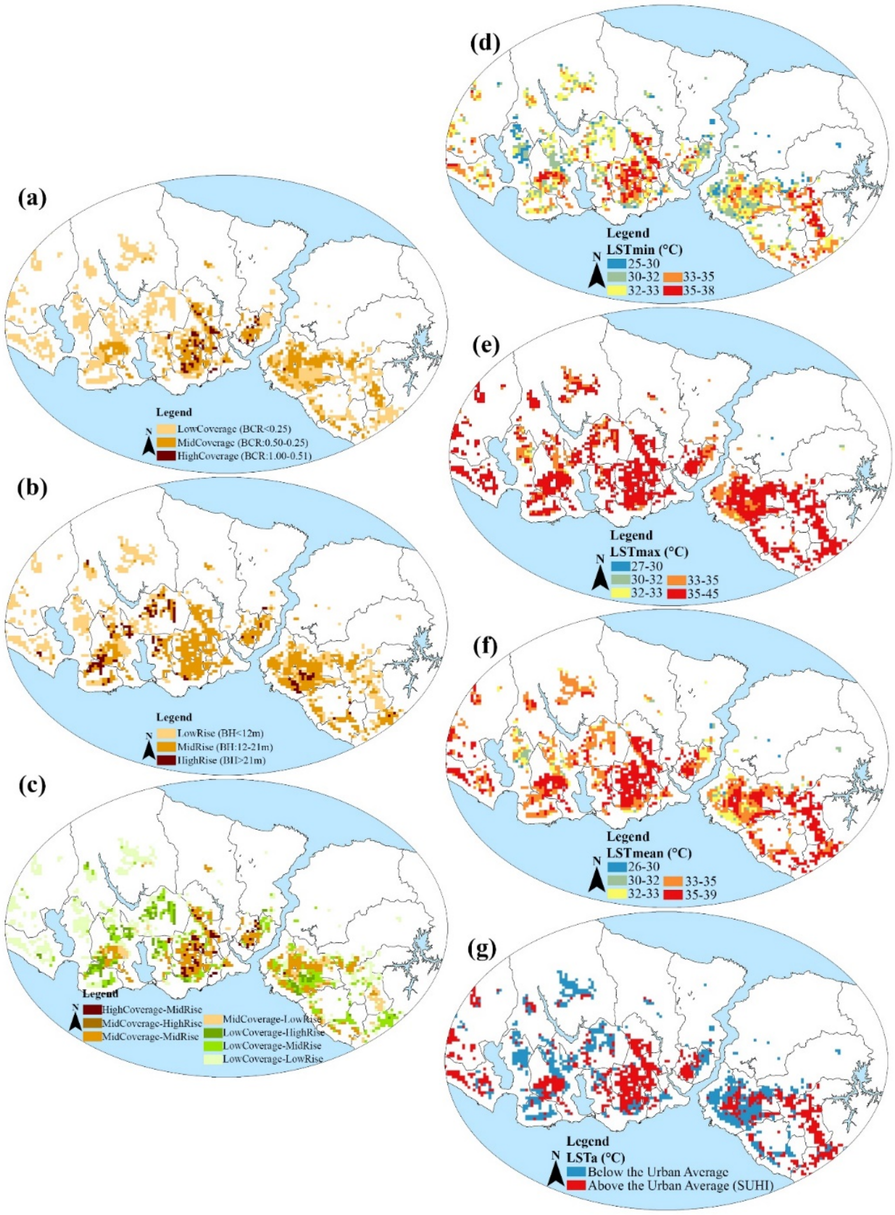

Appendix 1. Distribution of the UDM typologies (a), (b), (c) and LSTs of sample grid cells (d), (e), (f), (g) in Istanbul. (g) demonstrates the LSTa of sample grid cells regarding the average temperature of 34.73°C on 25th July 2017.

DOI: 10.15320/ICONARP.2022.220

	(I) Typologies	(J) Typologies	Mean Difference (I-J)	Std. Error	Sig.
GROUP-1: BC	HC	**MC**	**1.549***	0.199	0.000
		LC	**3.163***	0.193	0.000
	MC	**HC**	**-1.549***	0.199	0.000
		LC	**1.613***	0.076	0.000
	LC	**HC**	**-3.163***	0.193	0.000
		MC	**-1.613***	0.076	0.000
GROUP-2: BH	HR	**MR**	**-1.572***	0.158	0.000
		LR	**-0.790***	0.156	0.000
	MR	**HR**	**1.572***	0.158	0.000
		LR	**0.782***	0.078	0.000
	LR	**HR**	**0.790***	0.156	0.000
		MR	**-0.782***	0.078	0.000
GROUP-3: UDM	HCMR	MCHR	1,817	0,638	0,230
		MCMR	**1,539***	0,202	0,000
		MCLR	**1,566***	0,228	0,000
		LCHR	**3,786***	0,232	0,000
		LCMR	**3,092***	0,203	0,000
		LCLR	**3,106***	0,194	0,000
	MCHR	HCMR	-1,817	0,638	0,230
		MCMR	-0,277	0,614	1,000
		MCLR	-0,251	0,623	1,000
		LCHR	1,968	0,624	0,128
		LCMR	1,274	0,614	0,636
		LCLR	1,288	0,611	0,618
	MCMR	**HCMR**	**-1,539***	0,202	0,000
		MCHR	0,277	0,614	1,000
		MCLR	0,026	0,150	1,000
		LCHR	**2,246***	0,155	0,000
		LCMR	**1,552***	0,107	0,000
		LCLR	**1,566***	0,090	0,000
	MCLR	**HCMR**	**-1,566***	0,228	0,000
		MCHR	0,251	0,623	1,000
		MCMR	-0,026	0,150	1,000
		LCHR	**2,220***	0,188	0,000
		LCMR	**1,526***	0,151	0,000
		LCLR	**1,540***	0,140	0,000
	LCHR	**HCMR**	**-3,786***	0,232	0,000
		MCHR	-1,968	0,624	0,128
		MCMR	**-2,246***	0,155	0,000
		MCLR	**-2,220***	0,188	0,000
		LCMR	**-0,693***	0,156	0,003
		LCLR	**-0,680***	0,144	0,001
	LCMR	**HCMR**	**-3,092***	0,203	0,000
		MCHR	-1,274	0,614	0,636
		MCMR	**-1,552***	0,107	0,000
		MCLR	**-1,526***	0,151	0,000
		LCHR	**0,693***	0,156	0,003
		LCLR	0,013	0,092	1,000
	LCLR	**HCMR**	**-3,106***	0,194	0,000
		MCHR	-1,288	0,611	0,618
		MCMR	**-1,566***	0,090	0,000
		MCLR	**-1,540***	0,140	0,000
		LCHR	**0,680***	0,144	0,001
		LCMR	-0,013	0,092	1,000

*The mean difference is significant at the 0.05 level.

Appendix 2. Scheffé's post hoc test results for Groups of BC, BH and UDM.

REFERENCES

Alexander, E. R. (1993). Density measures: A review and analysis. Journal of Architectural and Planning Research, 181–202.

Arnfield, A. J. (1990a). Canyon geometry, the urban fabric and nocturnal cooling: a simulation approach. Physical Geography, 11(3), 220–239.

Arnfield, A. J. (1990b). Street design and urban canyon solar access. Energy and Buildings, 14(2), 117–131.

Arnfield, A. J. (2003). Two decades of urban climate research: a review of turbulence, exchanges of energy and water, and the urban heat island.

International Journal of Climatology, 23(1), 1–26.
Barsi, J., Schott, J., Hook, S., Raqueno, N., Markham, B., & Radocinski, R. (2014). Landsat-8 thermal infrared sensor (TIRS) vicarious radiometric calibration. Remote Sensing, 6(11), 11607–11626.
Basar, U. G., Kaya, S., & Karaca, M. (2008). Evaluation of urban heat island in Istanbul using remote sensing techniques. Commission VII, WG VII/5. The International Archives of the Photogrammetry, Remote Sensing and Spatial Information Sciences, 37.
Bektas Balcik, F. (2014). Determining the impact of urban components on land surface temperature of Istanbul by using remote sensing indices. Environmental Monitoring and Assessment, 186(2), 859–872. https://doi.org/10.1007/s10661-013-3427-5
Błażejczyk, K., Jendritzky, G., Bröde, P., Fiala, D., Havenith, G., Epstein, Y., … Kampmann, B. (2013). An introduction to the universal thermal climate index (UTCI). Geographia Polonica, 86(1), 5–10.
Bolen, F. (2004). Housing policy and housing systems in Turkey. A| Z ITU Journal of the Faculty of Architecture, 1(1), 14–31.
Ç.Ş.B. (2018). İstanbul İli 2017 Yılı Çevre Durum Raporu. Retrieved from https://ced.csb.gov.tr/2017-yili-il-cevre-durum-raporlari-i-85928
Chow, W. T. L., Brennan, D., & Brazel, A. J. (2012). Urban heat island research in Phoenix, Arizona: Theoretical contributions and policy applications. Bulletin of the American Meteorological Society, 93(4), 517–530.
Chun, B., & Guldmann, J.-M. (2014). Spatial statistical analysis and simulation of the urban heat island in high-density central cities. Landscape and Urban Planning, 125, 76–88.

Corburn, J. (2009). Cities, climate change and urban heat island mitigation: localising global environmental science. Urban Studies, 46(2), 413–427.
Dihkan, M., Karsli, F., Guneroglu, A., & Guneroglu, N. (2015). Evaluation of surface urban heat island (SUHI) effect on coastal zone: The case of Istanbul Megacity. Ocean & Coastal Management, 118, 309–316.
Erdem Okumus, D., & Terzi, F. (2021). Evaluating the role of urban fabric on surface urban heat island: The case of Istanbul. Sustainable Cities and Society, 73. https://doi.org/10.1016/j.scs.2021.103128
Ezber, Y., Sen, O. L., Kindap, T., & Karaca, M. (2007). Climatic effects of urbanization in Istanbul: a statistical and modeling analysis. International Journal of Climatology: A Journal of the Royal Meteorological Society, 27(5), 667–679.
Feng, X., & Myint, S. W. (2016). Exploring the effect of neighboring land cover pattern on land surface temperature of central building objects. Building and Environment, 95, 346–354.
Gago, E. J., Roldan, J., Pacheco-Torres, R., & Ordóñez, J. (2013). The city and urban heat islands: A review of strategies to mitigate adverse effects. Renewable and Sustainable Energy Reviews, 25, 749–758.
Giridharan, R., Lau, S. S. Y., Ganesan, S., & Givoni, B. (2007). Urban design factors influencing heat island intensity in high-rise high-density environments of Hong Kong. Building and Environment, 42(10), 3669–3684.
Guha, S., Govil, H., Dey, A., & Gill, N. (2018). Analytical study of land surface temperature with NDVI and NDBI using Landsat 8 OLI and TIRS data in Florence and Naples city, Italy. European Journal of Remote Sensing, 51(1), 667–678.
Guo, G., Zhou, X., Wu, Z., Xiao, R., & Chen, Y. (2016). Characterizing the impact of urban morphology heterogeneity on land surface temperature in

DOI: 10.15320/ICONARP.2022.220

Guangzhou, China. Environmental Modelling & Software, 84, 427–439.

Hamin, E. M., & Gurran, N. (2009). Urban form and climate change : Balancing adaptation and mitigation in the U . S . and Australia. Habitat International, 33(3), 238–245. https://doi.org/10.1016/j.habitatint.2008.10.005

He, B.-J., Ding, L., & Prasad, D. (2020a). Relationships among local-scale urban morphology, urban ventilation, urban heat island and outdoor thermal comfort under sea breeze influence. Sustainable Cities and Society, 60, 102289.

He, B.-J., Ding, L., & Prasad, D. (2020b). Urban ventilation and its potential for local warming mitigation: A field experiment in an open low-rise gridiron precinct. Sustainable Cities and Society, 55, 102028.

Hu, Y., White, M., & Ding, W. (2016). An urban form experiment on urban heat island effect in high density area. Procedia Engineering, 169, 166–174.

İ.B.B. (2018). İstanbul Büyükşehir Belediyesi İstanbul İklim Değişikliği Eylem Planı. Retrieved from https://www.iklim.istanbul/wp-content/uploads/FinalRaporu.pdf

IPCC. (2021). Climate Change 2021: The Physical Science Basis. Contribution of Working Group I to the Sixth Assessment Report of the Intergovernmental Panel on Climate Change. Retrieved from https://www.ipcc.ch/report/ar6/wg1/downloads/report/IPCC_AR6_WGI_Full_Report.pdf

IPCC. (2022). Climate Change 2022: Impacts, Adaptation and Vulnerability. Retrieved from https://www.ipcc.ch/report/ar6/wg2/

Jiménez-Muñoz, J. C., Sobrino, J., Gillespie, A., Sabol, D., & Gustafson, W. (2006). Improved land surface emissivities over agricultural areas using ASTER NDVI. Remote Sensing of Environment, 103(4), 474–487.

Jiménez-Muñoz, J. C., Sobrino, J., Plaza, A., Guanter, L., Moreno, J., & Martínez, P. (2009). Comparison between fractional vegetation cover retrievals from vegetation indices and spectral mixture analysis: Case study of PROBA/CHRIS data over an agricultural area. Sensors, 9(2), 768–793.

Kaya, S., Basar, U. G., Karaca, M., & Seker, D. Z. (2012). Assessment of urban heat islands using remotely sensed data. Ekoloji, 21(84), 107–113.

Keles, R. (1993). Kentleşme politikası. İmge Kitabevi.

Kleerekoper, L., Van Esch, M., & Salcedo, T. B. (2012). How to make a city climate-proof, addressing the urban heat island effect. Resources, Conservation and Recycling, 64, 30–38.

Knuth, S., Stehlin, J., & Millington, N. (2020). Rethinking climate futures through urban fabrics:(De) growth, densification, and the politics of scale. Urban Geography, 1–9.

Liao, W., Hong, T., & Heo, Y. (2021). The effect of spatial heterogeneity in urban morphology on surface urban heat islands. Energy and Buildings, 244, 111027.

Lin, P., Lau, S. S. Y., Qin, H., & Gou, Z. (2017). Effects of urban planning indicators on urban heat island: a case study of pocket parks in high-rise high-density environment. Landscape and Urban Planning, 168, 48–60.

M.G.M. (2022). General statistical data of the provinces. Retrieved 6 April 2022, from Turkish State Meteorological Service website: https://mgm.gov.tr/veridegerlendirme/il-ve-ilceler-istatistik.aspx?k=A&m=ISTANBUL

Masoumi, H. E., Terzi, F., & Serag, Y. M. (2019). Neighborhood-scale urban form typologies of large metropolitan areas: Observations on Istanbul, Cairo, and Tehran. Cities, 85, 170–186.

Metz, B., Berk, M., den Elzen, M., de Vries, B., & van Vuuren, D. (2002). Towards an equitable global climate change regime: compatibility with Article 2 of the Climate Change Convention and the link with sustainable development. Climate Policy, 2(2–3), 211–230.

Mirzaei, P. A., & Haghighat, F. (2010). Approaches to study urban heat island–abilities and limitations. Building and Environment, 45(10), 2192–2201.

Oke, T. R. (1981). Canyon geometry and the nocturnal urban heat island: Comparison of scale model and field observations. Journal of Climatology, 1(3), 237–254. https://doi.org/10.1002/joc.3370010304

Oke, T. R. (1982). The energetic basis of the urban heat island. Quarterly Journal of the Royal Meteorological Society, 108(455), 1–24.

Oke, T. R. (1987). Boundary layer climates. Routledge.

Oke, T. R., & Maxwell, G. B. (1975). Urban heat island dynamics in Montreal and Vancouver. Atmospheric Environment (1967), 9(2), 191–200.

Pomponi, F., Saint, R., Arehart, J. H., Gharavi, N., & D'Amico, B. (2021). Decoupling density from tallness in analysing the life cycle greenhouse gas emissions of cities. Npj Urban Sustainability, 1(1), 1–10.

Quattrochi, D. A., & Goel, N. S. (1995). Spatial and temporal scaling of thermal infrared remote sensing data. Remote Sensing Reviews, 12(3–4), 255–286.

Salvati, A., Roura, H. C., & Cecere, C. (2017). Assessing the urban heat island and its energy impact on residential buildings in Mediterranean climate: Barcelona case study. Energy and Buildings, 146, 38–54.

Santamouris, M. (2013). Using cool pavements as a mitigation strategy to fi ght urban heat island — A review of the actual developments. Renewable and Sustainable Energy Reviews, 26, 224–240. https://doi.org/10.1016/j.rser.2013.05.047

Santamouris, M., Ding, L., & Osmond, P. (2019). Urban Heat Island Mitigation. In Decarbonising the Built Environment (pp. 337–355). Springer.

Scheffe, H. (1953). A method for judging all contrasts in the analysis of variance. Biometrika, 40(1–2), 87–110.

Scheffe, H. (1959). The Analysis of Variance, New York: JohnWiley & Sons. SchefféThe Analysis of Variance1959.

Shishegar, N. (2013). Street Design and Urban Microclimate: Analyzing the Effects of Street Geometryand Orientation on Airflow and Solar Access in Urban Canyons. Journal of Clean Energy Technologies, 1(1).

Sobrino, J. A., Jiménez-Muñoz, J. C., & Paolini, L. (2004). Land surface temperature retrieval from LANDSAT TM 5. Remote Sensing of Environment, 90(4), 434–440.

Song, J., Chen, W., Zhang, J., Huang, K., Hou, B., & Prishchepov, A. V. (2020). Effects of building density on land surface temperature in China: Spatial patterns and determinants. Landscape and Urban Planning, 198, 103794.

Stewart, I. D., & Oke, T. R. (2012). Local climate zones for urban temperature studies. Bulletin of the American Meteorological Society, 93(12), 1879–1900.

Strømann-Andersen, J., & Sattrup, P. A. (2011). The urban canyon and building energy use: Urban density versus daylight and passive solar gains. Energy and Buildings, 43(8).

Sun, Y., Gao, C., Li, J., Wang, R., & Liu, J. (2019). Quantifying the effects of urban form on land surface temperature in subtropical high-density urban areas using machine learning. Remote Sensing, 11(8), 959.

Swart, R., Robinson, J., & Cohen, S. (2003). Climate change and sustainable development: expanding the options. Climate Policy, 3(sup1), S19–S40.

DOI: 10.15320/ICONARP.2022.220

Terzi, F., & Bolen, F. (2009). Urban sprawl measurement of Istanbul. European Planning Studies, 17(10), 1559–1570.

Terzi, F., & Bolen, F. (2012). The potential effects of spatial strategies on urban sprawl in Istanbul. Urban Studies, 49(6), 1229–1250.

U.N. (2015). Transforming Our World:The 2030 Agenda For Sustainable Development. Retrieved from https://sdgs.un.org/sites/default/files/publications/21252030 Agenda for Sustainable Development web.pdf

U.N. (2019). The strategic plan 2020-2023. Retrieved from UN Habitat website: https://unhabitat.org/sites/default/files/documents/2019-09/strategic_plan_2020-2023.pdf

U.N.D.P. (2015). Sürdürülebilir Kalkınma Amaçları. Retrieved from https://www.tr.undp.org/content/turkey/tr/home/sustainable-development-goals.html

USGS. (2019). Landsat 8 Data Users Handbook Version 5.0 November 2019. Nasa, 8(November), 97. Retrieved from https://landsat.usgs.gov/documents/Landsat8DataUsersHandbook.pdf

Voogt, James A, & Oke, T. R. (1997). Complete urban surface temperatures. Journal of Applied Meteorology, 36(9), 1117–1132.

Voogt, James A, & Oke, T. R. (1998). Effects of urban surface geometry on remotely-sensed surface temperature. International Journal of Remote Sensing, 19(5), 895–920.

Voogt, James A, & Oke, T. R. (2003). Thermal remote sensing of urban climates. Remote Sensing of Environment, 86(3), 370–384.

Voogt, James Adrian. (1995). Thermal remote sensing of urban surface temperatures. University of British Columbia.

Weng, Q. (2009). Thermal infrared remote sensing for urban climate and environmental studies: Methods, applications, and trends. ISPRS Journal of Photogrammetry and Remote Sensing, 64(4), 335–344.

Weng, Q., Lu, D., & Schubring, J. (2004). Estimation of land surface temperature–vegetation abundance relationship for urban heat island studies. Remote Sensing of Environment, 89(4), 467–483.

Wong, N. H., Jusuf, S. K., Syafii, N. I., Chen, Y., Hajadi, N., Sathyanarayanan, H., & Manickavasagam, Y. V. (2011). Evaluation of the impact of the surrounding urban morphology on building energy consumption. Solar Energy, 85(1), 57–71.

Xu, H., & Chen, B. (2004). Remote sensing of the urban heat island and its changes in Xiamen City of SE. Journal of Environmental Sciences, 16(2), 276–281.

Yang, F., Lau, S. S. Y., & Qian, F. (2010). Summertime heat island intensities in three high-rise housing quarters in inner-city Shanghai China: Building layout, density and greenery. Building and Environment, 45(1), 115–134.

Yang, Jun, Jin, S., Xiao, X., Jin, C., Xia, J. C., Li, X., & Wang, S. (2019). Local climate zone ventilation and urban land surface temperatures: Towards a performance-based and wind-sensitive planning proposal in megacities. Sustainable Cities and Society, 47, 101487.

Yang, Junyan, Shi, B., Xia, G., Xue, Q., & Cao, S.-J. (2020). Impacts of Urban form on Thermal Environment near the Surface Region at Pedestrian Height: A Case Study Based on High-density Built-up Areas of Nanjing City in China. Sustainability, 12(5), 1737.

Yang, X., & Li, Y. (2015). The impact of building density and building height heterogeneity on average urban albedo and street surface temperature.

Building and Environment, 90, 146–156.
Yilmaz, S., Irmak, M. A., & Qaid, A. (2022). Assessing the effects of different urban landscapes and built environment patterns on thermal comfort and air pollution in Erzurum city, Turkey. Building and Environment, 109210.
Yilmaz, S., Külekçi, E. A., Mutlu, B. E., & Sezen, I. (2021). Analysis of winter thermal comfort conditions: street scenarios using ENVI-met model. Environmental Science and Pollution Research, 28(45), 63837–63859.
Yin, C., Yuan, M., Lu, Y., Huang, Y., & Liu, Y. (2018). Effects of urban form on the urban heat island effect based on spatial regression model. Science of The Total Environment, 634, 696–704.
Zhao, C. (2018). Linking the local climate zones and land surface temperature to investigate the surface urban heat island, a case study of San Antonio, Texas, US. ISPRS Annals of Photogrammetry, Remote Sensing & Spatial Information Sciences, 4(3).
Zheng, Z., Zhou, W., Yan, J., Qian, Y., Wang, J., & Li, W. (2019). The higher, the cooler? Effects of building height on land surface temperatures in residential areas of Beijing. Physics and Chemistry of the Earth, Parts A/B/C, 110, 149–156.
Zhou, W., Huang, G., & Cadenasso, M. L. (2011). Does spatial configuration matter? Understanding the effects of land cover pattern on land surface temperature in urban landscapes. Landscape and Urban Planning, 102(1), 54–63.

Resume

Deniz Erdem Okumus is a faculty member in the City and Regional Planning Department at Yildiz Technical University. The area of interest focuses on urban climate, climate-responsive urban design, computational design approaches, urban informatics and GIS. Dr. Erdem-Okumus worked as a visiting researcher in the Chair of Design Informatics at Delft University of Technology, The Netherlands in 2021.

Fatih Terzi is a faculty member in the Department of Urban and Regional Planning at Istanbul Technical University. The area of interest focuses on sustainable urban development, climate responsive design, and eco-smart cities. Fatih Terzi paid a visit to Clemson University, SC, USA, in 2004; the Center for Advanced Spatial Analysis Center (CASA), University College London, in 2008; and the Technology and Community Research Center of the Technical University Berlin in 2017 as a guest researcher.

DOI: 10.15320/ICONARP.2022.220